



*Envelope system composed of 3D printed blocks exploiting a honeycomb shape.*

# 3D printed concrete blocks made with sustainable recycled material

Stelladriana Volpe<sup>1</sup>, Valentino Sangiorgio<sup>2\*</sup>, Andrea Petrella<sup>1</sup>, Michele Notarnicola<sup>1</sup>, Humberto Varum<sup>3</sup>, and Francesco Fiorito<sup>1</sup>

<sup>1</sup>Dipartimento di Ingegneria Civile, Ambientale, del Territorio, Edile e di Chimica, Politecnico di Bari.

<sup>2</sup>Department of Engineering and Geology, University G. D'Annunzio of Chieti-Pescara.

<sup>3</sup>Faculdade de Engenharia da Universidade do Porto.

Email: \*valentino.sangiorgio@unich.it

**Abstract:** The use of recovered materials in building construction is one of the most effective strategies for reducing the environmental impacts of the construction sector. Innovative technologies such as 3D construction printing can be applied in combination with recycling strategies in order to optimise their performances also from an environmental point of view. In fact, several studies have proposed the processing of waste material into printable material. At the same time, performance studies must be conducted on the building components produced by these methods. This study proposes a methodological approach to design a 3D printable building component made with recycled materials considering the improvement of thermal performances. In particular, the approach is based on three steps: reuse strategy conception; target performance definition, modelling and iterative simulation; 3D printing setting. The methodological approach has been applied to a 3D printable block using as printable material a cement-based mortar with recycled aggregates and recycled insulating material. As a result, the component's shape (interlocking and inspired by honeycombs) can be customised to achieve the required thermal performance by using recycled materials in the printing process.

**Keywords:** 3D construction printing; recycled material; thermal performances; building envelope; technical architecture; building innovation and digitization.

**Cite as:** Volpe, S., Sangiorgio, V., Petrella, A., Notarnicola, M., Varum, H., and Fiorito, F. 2023. '3D printed concrete blocks made with sustainable recycled material'. *VITRUVIO - International Journal of Architectural Technology and Sustainability*, 8(special issue), pp.70-83. <https://doi.org/10.4995/vitruvio-ijats.2023.18832>

## 1. Introduction

In the last decades, the scientific and technical world is facing the critical issue of waste production and energy demand for buildings and infrastructures. Indeed, responsible consumption and production are one of the goals of Agenda 2030 to reduce waste generation through prevention, reduction, recycling and reuse (Colglazier, 2015). A significant amount of waste is produced using traditional construction methods. In addition, both the construction and demolition processes require high consumption of resources. The increasing costs of raw materials both in terms of economic and environmental impact are affecting the wide spectrum sustainability of building constructions. Yilong *et al.*, identified one of the possible causes of the carbon-dioxide emissions (and consequently of the unsustainability of the constructions) in the huge demand for concrete (Han, 2020). Consequently, the upgrading of the construction industry through innovative construction processes is becoming an essential need. New technologies and more efficient management of resources (considering material reuse and recycling) is the substantial innovation that the construction sector requires.

Recently, the possibility of revolutionizing construction processes is offered by the advent of additive manufacturing technology. In particular, additive manufacturing is able to achieve lower costs, reduce waste, and simplify the supply chain. Moreover, such a promising technology is particularly effective in the use of recycled materials typically used in printable mixtures (Ding *et al.*, 2020).

Even if additive manufacturing is a promising technology, some drawbacks need to be addressed. One of the major challenges concerns the achievement of adequate printing requirements using materials with suitable rheological, extrudability and buildability characteristics. To achieve this performance, many of the mixtures used in additive manufacturing are currently based on Portland cement and fine aggregates, which requires high production energy with subsequent high amounts of CO<sub>2</sub> emissions (Tinoco *et al.*, 2022).

Different types of 3D printing admixtures have been investigated to include recycled materials as components, on the other hand, there are still few evaluations involving a largely recycled mixture. Pozzolanic materials can be used to partially replace cement and to obtain improved characteristics such as high-early strength, high workability, low porosity and corrosion resistance. Moreover, some studies included by-product materials as additives in the cement admixture. To provide some examples, silica fume is a by-product in the production of silicon and ferrosilicon alloys (Ahmad and Chen,

2018; Xu *et al.*, 2020); fly ash is a by-product of coal combustion in thermal power plants (Jianming *et al.*, 2020; Liu *et al.*, 2019; Panda *et al.*, 2019; Sun *et al.*, 2019); rice husk ash derives from rice husks, which are usually regarded as agricultural waste (Muthukrishnan *et al.*, 2020). Other authors investigated the possibility of replacing all or part of natural aggregates with recycled aggregates deriving from construction and demolition solid waste (Liu *et al.*, 2022; Qian *et al.*, 2022; Zhang and Xiao, 2021). Another promising recycled technique involves the use of reused sand for concrete 3D printing to reduce costs and the environmental impact (but it is still at the early stage of exploration) (Han *et al.*, 2021). Other possible substitutes of aggregates to reach a more sustainable 3D printable concrete can be found in recycled brick aggregate (Christen *et al.*, 2022); glass cullets (Ting *et al.*, 2021) or natural fibres (le Duigou *et al.*, 2020).

Finally, the reused materials can be effectively applied for thermal insulation in traditional buildings. Indeed, plastic and glass have been widely used to produce recycled insulating panels or filler insulation material (Majumder *et al.*, 2021). Such a “reuse” approach can be proposed also for the insulation of 3D printed building blocks. In particular, fine-grained or loose materials can be effectively integrated into the 3D printing blocks directly during the printing process. In addition, the advent of automation in construction will allow this integration automatically. To sum up, even if the study of recycled materials for 3D printing is widely faced in the related literature, few examples are present in related literature of 3D printed components made with sustainable recycled material. Moreover, the used methodological approaches do not exploit the synergy between parametric design, and performance simulation to adjust the geometrical configuration of the 3D printed components.

The current work proposes a three-step methodological approach to designing an effective 3D printed building block exploiting an interlocking shape inspired by honeycombs.

In addition, the proposed block includes reused material in both the printing admixture and the insulation layer. Firstly, the reuse design is defined by selecting processes to recover the material, secondly, parametric modelling and simulation are achieved to optimise the shape of the component and thirdly the best printing setting for additive manufacturing is identified. The proposed approach is applied to design prefabricated interlocking 3D printed blocks exploiting a honeycomb shape. The reused material is both in the printable material (a mortar including recycled glass or rubber) and insulation layer (made with cellulose).

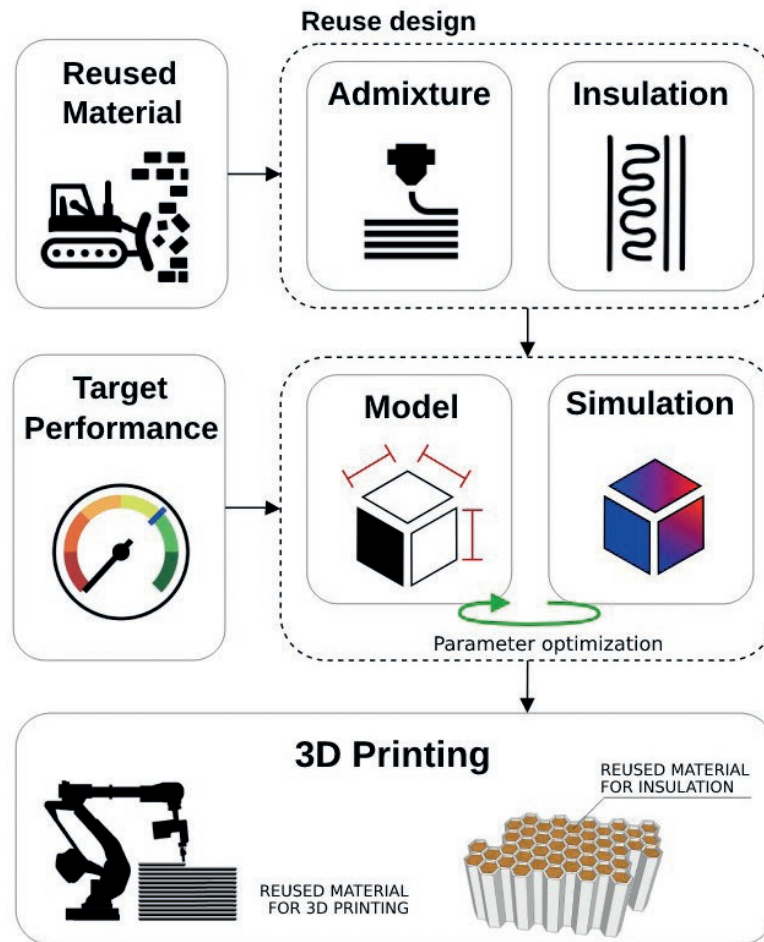


Figure 1 | Overview of the proposed methodology.

## 2. Methodology

The proposed methodology is based on three steps (Fig. 1) of using recycled materials to create 3D printed building components.

1. Reuse strategies design.
2. Target performance definition, parametric modelling, iterative simulation and performance optimisation.
3. 3D printing setting.

### 2.1 Reuse strategies design

The first phase of the method concerns the conception of the reuse strategy. Construction and demolition wastes represent a massive portion of global waste production. This type of waste is suitable for reuse or recycling to produce secondary raw materials due to the

large volumes and low toxicity. During the reuse strategy phase, intervention or demolition techniques can be defined and a list of possible reusable components and recyclable materials can be set. Generally, the recyclable fractions of construction and demolition waste are stone, ceramic, glass, wood and metal. Possible reuse strategies for such waste material regard the inclusion of recycled material as aggregates in concrete conglomerates and the transformation of waste into thermal insulating materials (Jeffrey 2011; de Andrade Salgado, 2022).

Subsequently, the possibility of implementing material from the defined demolition waste in 3D printable material can be investigated. This opportunity depends also on the rheological characteristics that the printed material should fulfil. Such rheological requirements of the material have been investigated in previous studies. The following are some conditions according to Bos *et al.*:

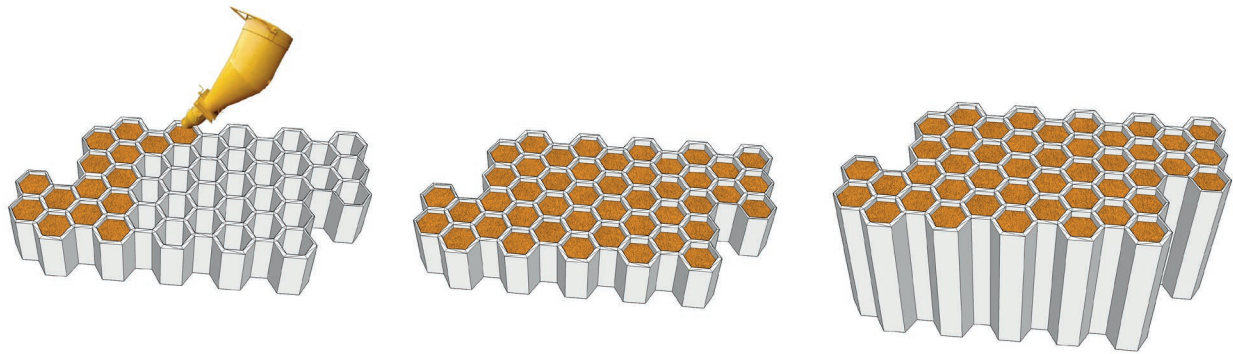


Figure 2 | Inclusion of insulating material during the 3D printing process.

- the initial yield stress must be greater than  $gh_0$  where  $g$  is the gravitational acceleration.
- Yield stress in the bottom layer must be greater than  $\rho gH/\sqrt{3}$  where  $\rho$  is the material density.
- Initial shear elastic modulus must be higher than  $\rho g h_0 / e_{tol}$  where  $e_{tol}$  is the tolerable deformation of the layer.
- Young elastic modulus must be higher than  $3\rho gH^3/2d^2$  (Roussel, 2018).

Another possibility to evaluate concerns the inclusion of waste material with thermal properties in the printing element. The insertion can be done by including insulating material in the printing mixture or as an insulating filler. The insulating filler can be inserted during or after the printing phase considering the internal geometry complexity and the type of consistency. In fact, if the geometry of the printed component is not complex and the insulation layer is made of loose material, the voids can be filled after the whole printing. On the contrary, the insulation material can be included by stopping the print after some layers to insert the insulating material filling the voids correctly (Fig. 2). Currently, such operation is planned manually but it can be automated using collaborative robots in construction.

## 2.2 Target performance definition

The expected component performance depends on the purpose of the designed element, on the boundary condition and on the intended use. Then a target performance that satisfies both the minimum regulatory standards and the user's comfort can be defined.

## 2.3 Parametric modelling

The conceptual design of the component needs to be clearly defined before proceeding to parametric modelling. In specific, the required functions, the integration of building services and the required performances in terms of both thermal protection and structural integrity should be specified. Also, the conceptual design must respect the current limits of available technologies in the realisation of complex geometric shapes (Sangiorgio, 2022).

Once the conceptual design has been defined, parametric modelling can be carried out. Parametric modelling supports the construction of geometry by exploiting mathematical equations managed with visual scripting. The tool makes it possible to immediately change the shape of the model geometry changing the values of certain parametrised dimensions. Consequently, once the conceptual design of the model is ready, all values of dimensions that need to be parameterised (e.g. thicknesses, lengths, heights, internal fills) need to be identified. The parameterisation of specific geometric characteristics (e.g. insulation thickness) lays the foundation for the subsequent optimisation of the component's performance in the subsequent simulation and iteration phase.

## 2.4 Iterative simulation

With the iterative simulation phase, the model parameters can be optimised. Finite Element Method (FEM) analysis used in synergy with parametric modelling can evaluate performance and iteratively modify specific geometric parameters to achieve the target performance. FEM is a numerical procedure that can be used to obtain solutions to a wide range of engineering problems involving stress analysis, dynamic analysis, electromagnetics and thermal problems useful for the proposed application

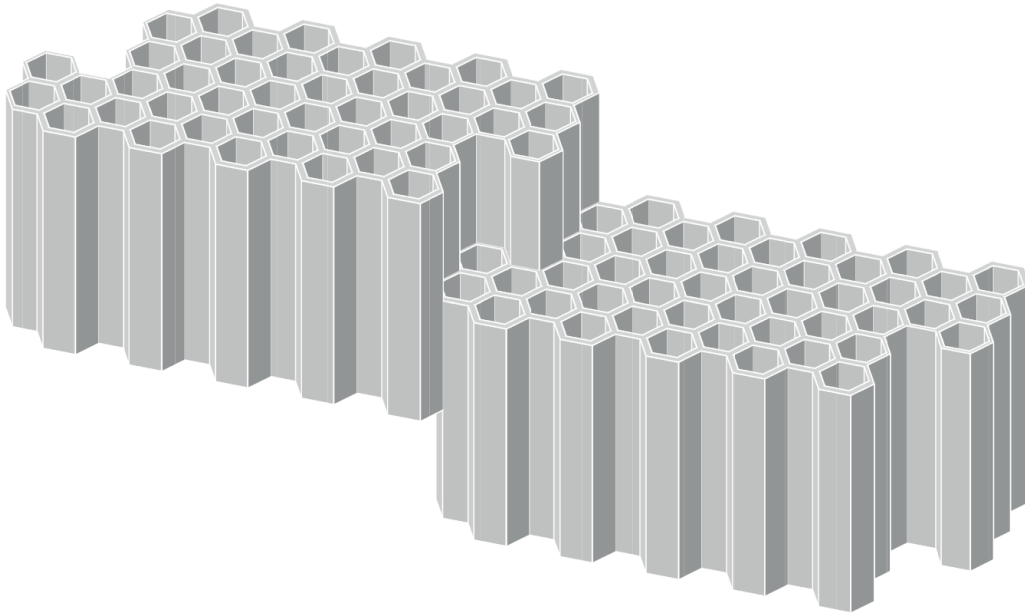


Figure 3 | 3D printable block with honeycomb geometry and possible assembly system.

(del Coz Díaz, 2006). In the proposed method, FEM is used in synergy with parametric modelling by setting up an iterative procedure. The objective is to identify the best parameter to meet minimum regulatory standards and user comfort in relation to thermal behaviour.

### 2.5 3D printing setting

During the 3D printing phase, an essential methodological step concerns the improvement of printability and the possible optimisation of the extrusion path. A uniform product quality requires the conversion of the element shapes in a continuous extrusion path. At the same time, a complex geometry does not always allow for a continuous 3D printing process. In this case, it is necessary to customise the slicing and g.code to achieve effective printing with limited inaccuracies (for example minimising the extrusion path overlapping) (Volpe, 2021).

## 3. Case study

The case study concerns the application of the proposed methodology to the design of an envelope block system consisting of 3D printable modular elements. The designed shape is based on a hexagonal pattern that can be easily produced with 3D printing technology. The elements' geometry allows on one hand the mutual interlocking and on the other hand the filling of the hexagonal cells with insulating material, increasing the thermal

performance. Starting from the described concept, the objective is to adapt the geometrical and material parameters in order to achieve the thermal performance of a specific climatic condition.

### 3.1 Reuse design

The reuse strategy of the case study considers the use of recycled materials as aggregates for the cementitious printing mixture and the use of recycled insulating material.

The cementitious materials evaluated consist of Magnesium Potassium Phosphate Cement (MKPC) prepared using aggregates of glass or rubber. These innovative cement-based mortars have been proposed in a previous study (Volpe, 2021). The MKPC components are magnesium oxide (MgO), potassium dihydrogen phosphate (KDP), borax, fly ash (FA), silica fume (SF) and water. The two different printing mixtures considered in the case study are MKPC with recycled expanded glass (0.5–1 mm), and MKPC with rubber granulate (0.5–1 mm) from tyre casings.

Expanded glass can be produced using a fraction of glass that cannot be reused in the glass manufacturing industry. In fact, while glass is particularly effective in a continuous recycling cycle without loss of quality, not the entire glass waste can be recycled for this purpose (Adhikary, 2021).



Rubber in general has problems with disposal and recycling due to the difficulty of polymeric materials in decomposition. The rubber from which tyres are made can be valorised as reusable material. Indeed, tyres can be turned into powders of different sizes, separated into groups and applied as reused materials in several contexts. A possible application concerns the production of sustainable concrete or mortars using rubber granulates as aggregates (Medina, 2017; Adhikari, 2000).

The lightweight aggregate-based mortars also have the advantage of increasing the thermos-insulating performance of the printed element. In fact, both MKPC typologies have been experimentally evaluated to assess their thermal properties. The thermal test has been conducted on cylindrical specimens (dimensions: 10 cm diameter and 5 cm height). ISOMET 2104 device (Applied Precision Ltd., Bratislava, Slovakia) was used to perform the thermal behaviour measurements inducing a constant heat flow through a heating probe, applied to the surface of the sample, and recording the temperature during the time period. The comparison of the experimental temperature values and the analytical solution of the heat conduction equation allows for obtaining the results. Table 1 shows the results of the thermal characteristics: the thermal conductivity  $\lambda$  (W/mK); the thermal diffusivity  $a$  ( $m^2/s$ ), that is the ratio between heat transferred and the volume heat capacity; the specific heat of the material  $c_p$  (J/kgK) and the average temperature  $t_m$  ( $^{\circ}C$ ).

The input data related to the two types of printing admixture in the subsequent thermal analysis simulation are respectively density equal to  $950 \text{ kg/m}^3$  and thermal conductivity equal to  $0.16 \text{ W/mK}$  for MKPC with expanded glass; density equal to  $1120 \text{ kg/m}^3$  and thermal conductivity equal to  $0.20 \text{ W/mK}$  for MKPC with tyre rubber granulate.

The filling material of the hexagonal cell has been evaluated as cellulose insulation. This type of loose insulation can be simply blown inside the cell after the 3D printing production phase. The high level of sustainability of this material derives from the use of recycled paper for

its production. From a thermal point of view, cellulose has a good insulating capacity due to its low density (approximately  $40 \text{ kg/m}^3$ ). As a consequence, the thermal conductivity is estimated at  $0.04 \text{ W/mK}$  (Lopez Hurtado, 2016). These parameters constitute input data in the subsequent thermal analysis simulation.

### 3.2 Target performance

The target performance refers to specific boundary conditions. The location chosen is the Apulian region (Italy), that according to the Italian Ministerial Decree (DM) No. 162 of 26 June 2015, corresponds to a climatic zone C. Depending on the different climate zones, external walls must meet a thermal transmittance limit value specified in the above-mentioned regulations. This thermal transmittance limit has then been considered the target performance for the case study. Therefore, the objective of the thermal analysis and the geometrical and material parameters variation is to achieve a thermal transmittance less than or equal to  $0.34 \text{ W/m}^2\text{K}$ .

### Model parameters definition

As described, the design concept is to create an external envelope element based on a hexagonal motif. The specific characteristics of the element may vary depending on the application conditions e.g. the climate zone, the intended use of the building etc. Consequently, at this stage, the methodology involves not only the design and modelling of the component but also the definition of variable parameters. In the current research, the defined variable geometric parameters are the number of hexagonal cells (with a total block thickness from 21 to 26 cm), the size of the hexagonal cells and the wall thickness. On the contrary, the block height of 20 cm and the block width of 40 cm are kept constant. The materials used as 3D printing admixtures also constitute a parameter of variation (printing material conductivity) for subsequent thermal analyses, while the defined insulating material is constant. Fig. 4 shows the dimensions constant or parametrised of the 3D model.

**Table 1** | Thermal characteristics of MKPC sample containing recycled expanded glass (MKPC<sub>glass</sub>) and MKPC sample containing tyre rubber granulate (MKPC<sub>rubber</sub>).

|                               | MKP <sub>Cglass</sub> | MKPC <sub>rubber</sub> |
|-------------------------------|-----------------------|------------------------|
| Conductivity $\lambda$ W/mK   | 0.16                  | 0.20                   |
| Diffusivity $a$ $m^2/s$       | 0.46                  | 0.17                   |
| Specific heat $c_p$ J/kgK     | 1.07                  | 1.18                   |
| Temperature $t_m$ $^{\circ}C$ | 32.05                 | 32.52                  |

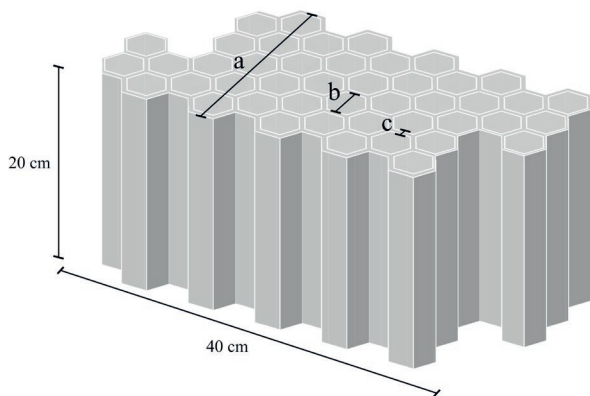


**Figure 4** | Constant and variable geometrical parameters of the 3D printable envelope block: (a) the number of hexagonal cells; (b) hexagonal cell size; (c) wall thickness

### 3.3 Simulation and iterations

The thermal analysis has been performed using ANSYS R22 software as steady-state thermal analysis. The simulation evaluates the heat transfer from a surface with a higher temperature to another surface with a lower

temperature. In fact, each different 3D model has been analysed defining the inner surface, at a temperature of 20°C, and the external surface, at a temperature of 0°C. The other surfaces, that have a symmetrical heat exchange because of the contact with other elements, have been considered adiabatic boundaries. Each material has been defined and then associated with the corresponding volume. The simulation returns results concerning the temperature variation along the heat path, the total heat flux and the directional heat flux along the orthogonal axis to the surfaces at different temperatures. By dividing the heat flux by the temperature gradient, the thermal transmittance of the element was estimated.

### 3.4 Results and discussion

Twenty-four different models have been analysed in order to achieve the required performance varying the parameters.

Table 2 contains the analysed models and related variation parameters.

Table 3 collects the resulting heat fluxes of each model and the relative thermal transmittance.

**Table 2** | Models and related variation parameters.

|   | Hexagon Number | Hexagon size [mm] | Wall thickness [mm] | Printing material |
|---|----------------|-------------------|---------------------|-------------------|
| A | 5              | 45                | 5                   | MKPCglass         |
| B | 5              | 45                | 5                   | MKPCrubber        |
| C | 5              | 40                | 10                  | MKPCglass         |
| D | 5              | 40                | 10                  | MKPCrubber        |
| E | 6              | 35                | 5                   | MKPCglass         |
| F | 6              | 35                | 5                   | MKPCrubber        |
| G | 6              | 30                | 10                  | MKPCglass         |
| H | 6              | 30                | 10                  | MKPCrubber        |
| I | 7              | 28.3              | 5                   | MKPCglass         |
| J | 7              | 28.3              | 5                   | MKPCrubber        |
| K | 7              | 23.3              | 10                  | MKPCglass         |
| L | 7              | 23.3              | 10                  | MKPCrubber        |
| M | 4              | 45                | 5                   | MKPCglass         |
| N | 4              | 45                | 5                   | MKPCrubber        |
| O | 4              | 40                | 10                  | MKPCglass         |
| P | 4              | 40                | 10                  | MKPCrubber        |
| Q | 5              | 35                | 5                   | MKPCglass         |
| R | 5              | 35                | 5                   | MKPCrubber        |
| S | 5              | 30                | 10                  | MKPCglass         |
| T | 5              | 30                | 10                  | MKPCrubber        |
| U | 6              | 28.3              | 5                   | MKPCglass         |
| V | 6              | 28.3              | 5                   | MKPCrubber        |
| W | 6              | 23.3              | 10                  | MKPCglass         |
| X | 6              | 23.3              | 10                  | MKPCrubber        |



**Table 3** | Models' results: heat fluxes and the relative thermal transmittance.

| Model | Heat flux [W/m <sup>2</sup> ] | Thermal transmittance [W/m <sup>2</sup> K] |
|-------|-------------------------------|--|
| A     | 5.64                          | 0.28                                       |
| B     | 6.71                          | 0.34                                       |
| C     | 5.48                          | 0.27                                       |
| D     | 6.49                          | 0.32                                       |
| E     | 6.34                          | 0.32                                       |
| F     | 7.55                          | 0.38                                       |
| G     | 6.15                          | 0.31                                       |
| H     | 8.15                          | 0.41                                       |
| I     | 5.97                          | 0.30                                       |
| J     | 7.02                          | 0.35                                       |
| K     | 6.37                          | 0.32                                       |
| L     | 7.54                          | 0.38                                       |
| M     | 6.95                          | 0.35                                       |
| N     | 8.26                          | 0.41                                       |
| O     | 6.72                          | 0.34                                       |
| P     | 7.96                          | 0.40                                       |
| Q     | 7.56                          | 0.38                                       |
| R     | 9.01                          | 0.45                                       |
| S     | 7.28                          | 0.36                                       |
| T     | 8.63                          | 0.43                                       |
| U     | 6.92                          | 0.35                                       |
| V     | 7.29                          | 0.36                                       |
| W     | 7.03                          | 0.35                                       |
| X     | 8.26                          | 0.41                                       |

The overall transmittance decreases proportionally with increasing cell size. This is due to an increase in the overall volume of the insulating material with lower thermal conductivity. As can be expected, even if the thickness of the material layer is reduced, the thermal behaviour improves moderately. The internal honeycomb cell configuration increases the heat path from the inner surface at a higher temperature to the outer surface at a lower temperature. In fact, the temperature distribution (Fig. 5 a) varies almost linearly along the heat flux direction. On the other hand, the Heat flux (Fig. 5 b) distribution clearly shows the heat path of lower thermal resistance due to the different materials and relative different conductivities.

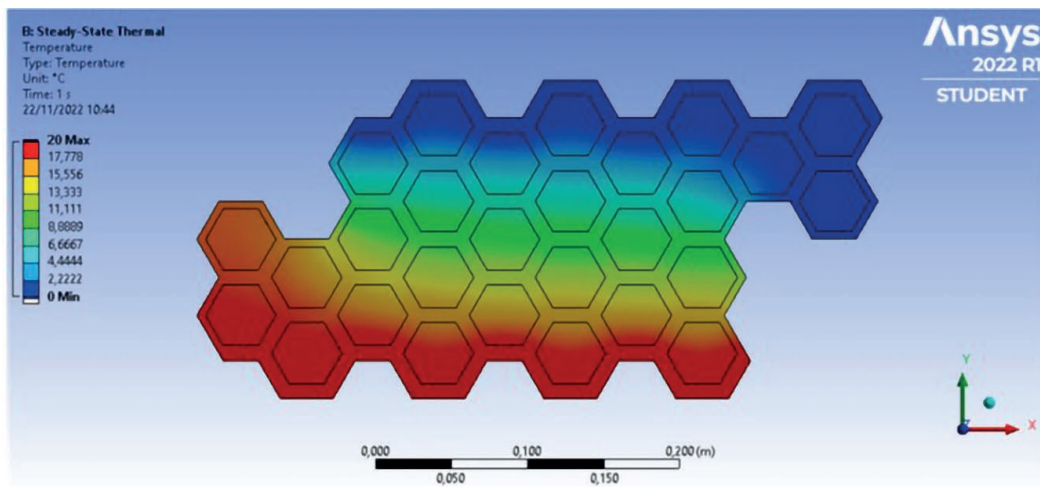
A multilinear regression analysis has been performed in order to estimate the relationship between the independent variables and the thermal transmittance. The resulting equation of the model is reported below:

$$y = 0.719 - 0.056 x_1 - 7.644 x_2 - 6.931 x_3 + 1.435 x_4$$

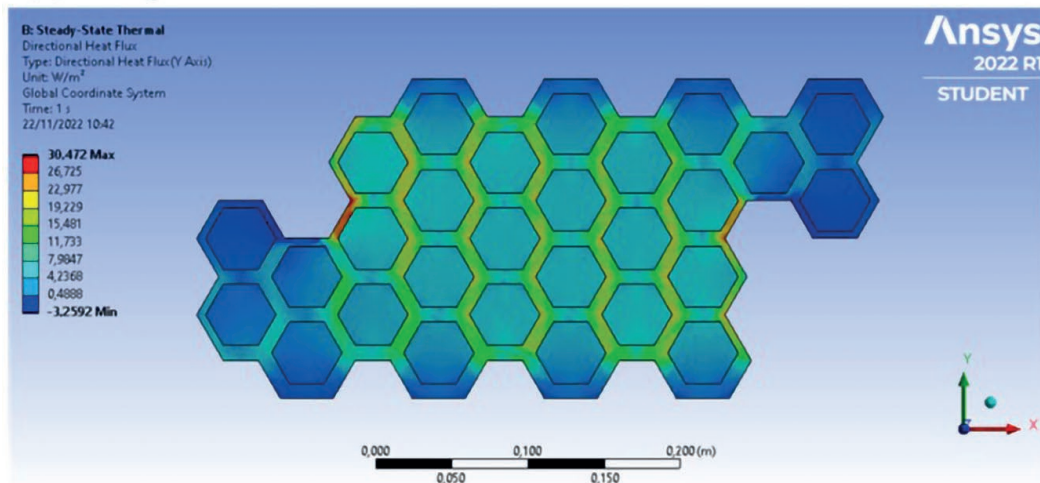
- y = thermal transmittance;
- x<sub>1</sub> = hexagon number;

- x<sub>2</sub> = hexagon dimension;
- x<sub>3</sub> = wall thickness;
- x<sub>4</sub> = printing material conductivity.

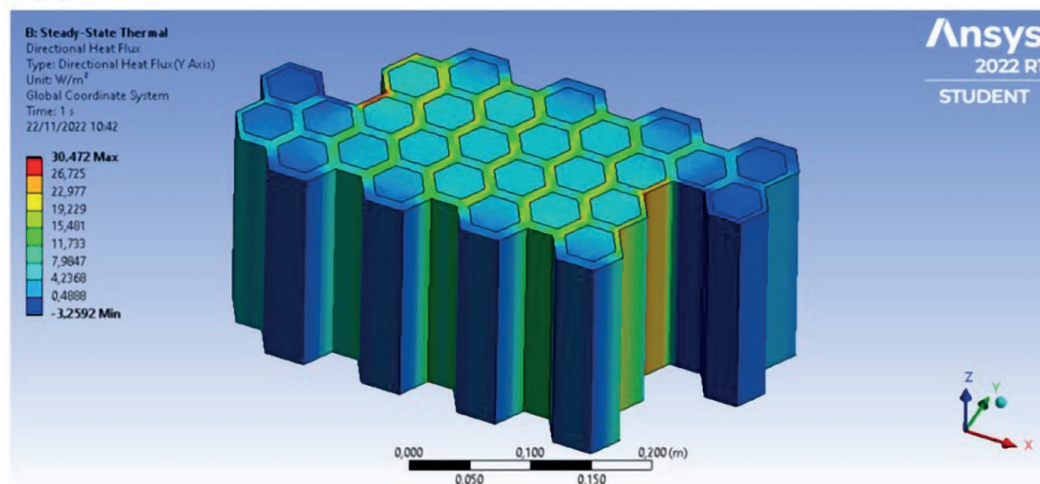
Although the models are characterised by different parameters, the relationship of the analysis results to the thickness of the insulating part of the blocks, which is one of the most influential factors, can be observed. In this regard, Fig. 6 shows the correlation between thermal transmittance and total insulation thickness that is given by the product of the hexagonal cell size by the number of hexagonal cells. Each point represents a model with a different parametric configuration. Each point series represents the variation in transmittance as insulation thickness increases while holding constant the printing material (thus the relative conductivity) and the wall thickness. The linear trendlines of the four series of points are indicated and, as visible, the slope is the same for each one. By decreasing the wall thickness, the trendline tends to translate horizontally as a lower wall thickness increases the space occupied by thermal insulation. Instead, by varying the conductivity of the printing material, the trendline shifts vertically.



(a) Temperature distribution



(b) Heat flux



(c) 3D view of heat flux

Figure 5 | Thermal analysis results of model O: (a) temperature distribution; (b) heat flux; (c) 3D view of heat flux.

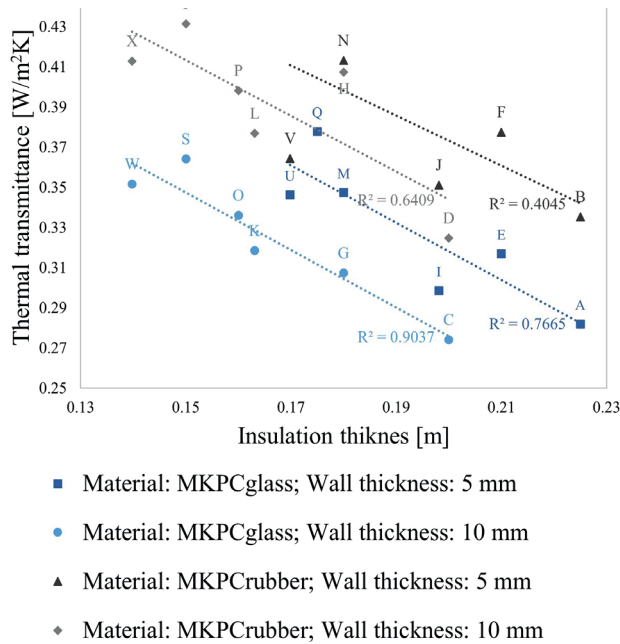


Figure 6 | Correlation between thermal transmittance and total insulation thickness of four model types.

As can be seen in the results, models B and O, containing rubber and glass aggregates respectively, have the thermal transmittance values closest to the reference value chosen (0.34 W/m²K). Consequently, the configuration can be implemented to constitute the external block wall in the climatic zone of the case study. In fact, together with finishing elements to complete the external and internal surfaces and make them plane, the thermal transmittance value of the entire envelope can be considered lower than the limit.

### 3.5 3D printing prototype

To verify the printability of the proposed shape, a prototype has been achieved in the Laboratories of the Polytechnic of Bari. The proposed model has been prototyped in scale within a printing test (Fig. 7) using clay as printing material. More in detail the model was reproduced to a scale of 1:10 using a Delta Wasp 40100 in the laboratory “FabLab Poliba” of the Polytechnic of Bari. The 3D printed model has demonstrated the feasibility of the designed geometry. Indeed, the extrusion does not incur common printing errors (Sangiorgio et al. 2022), and the printed shape is achieved without deformation reflecting the 3D digital model.

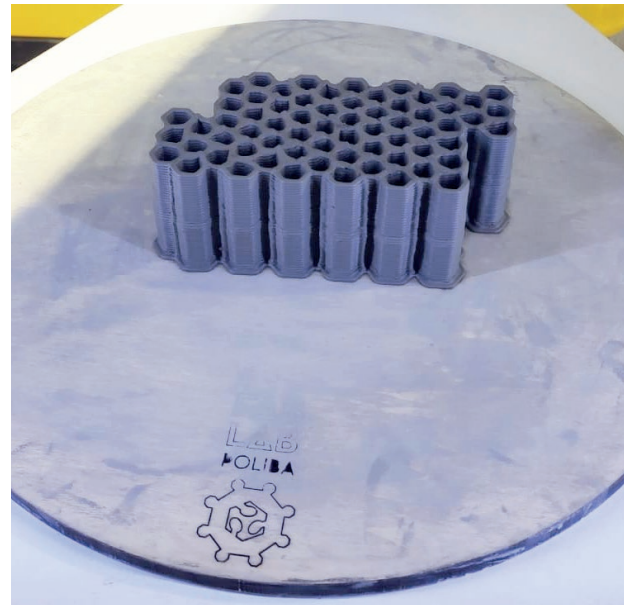


Figure 7 | 3D Printing test in the FabLab Poliba of the Polytechnic of Bari.

## 4. Conclusions

3D construction printing constitutes a promising technology to combine recycled materials and novel geometries. The present work proposes a methodology to design building components with effective performance printable using reused materials. The methodology has been applied to a case study consisting of a building block envelope with a honeycomb geometry. Through the methodological approach, the envelope block has been thermally optimised by varying geometric and material parameters with respect to specified boundary conditions. In particular, two different printing admixtures have been evaluated. Both cement-based materials (MKPC) contain recycled aggregates made with expanded glass or tyre rubber granulate. The lightweight aggregate-based mortars have thermal properties investigated through experimental tests. As a filling material for the hexagonal cell, cellulose insulation has been proposed. The parametric models have been analysed with FEM simulations demonstrating the potential of 3D printing technology combined with reused materials. Indeed, one model configuration for each printing admixture evaluated reaches the thermal transmittance limit of the climatic zone chosen. Future research will investigate both the combination of structural and thermal performances by automating the simulations and iterative parameter optimisation process to obtain an effective design system for 3D printed components with recycled materials.

## Acknowledgement

This research was funded by the European Union – European Social Fund – PON Research and Innovation 20214- 2020.

A special thanks is addressed to FabLab Bitonto for supporting the development of the prototype in the laboratory “Fablab Poliba”.

## Authors' contribution

Stelladriana Volpe: conceptualization, methodology, investigation, validation, visualization, formal analysis, data curation, writing – original draft preparation.

Valentino Sangiorgio: conceptualization, methodology, investigation, validation, visualization, formal analysis, data curation, writing - original draft preparation.

Andrea Petrella: laboratory test.

Michele Notarnicola: laboratory test.

Humberto Varum: conceptualization, review and editing, supervision.

Francesco Fiorito: conceptualization, review and editing, supervision.

All authors have read and agreed to the published version of the manuscript.

## References

- Adhikari, B., De, D., Maiti, S., (2000). Reclamation and recycling of waste rubber. *Prog Polym Sci* 25, 909–948. [https://doi.org/10.1016/S0079-6700\(00\)00020-4](https://doi.org/10.1016/S0079-6700(00)00020-4)
- Adhikary, S.K., Ashish, D.K., Rudžionis, Ž., (2021). Expanded glass as light-weight aggregate in concrete – A review. *J Clean Prod* 313, 127848. <https://doi.org/10.1016/J.JCLEPRO.2021.127848>
- Ahmad, M.R., Chen, B., (2018). Effect of silica fume and basalt fiber on the mechanical properties and microstructure of magnesium phosphate cement (MPC) mortar. *Constr Build Mater* 190, 466–478. <https://doi.org/10.1016/J.CONBUILDMAT.2018.09.143>
- Christen, H., van Zijl, G., de Villiers, W., (2022). The incorporation of recycled brick aggregate in 3D printed concrete. *Cleaner Materials* 4, 100090. <https://doi.org/10.1016/J.CLEMA.2022.100090>
- Colglazier, W., (2015). Sustainable development agenda: 2030. *Science* (1979) 349, 1048–1050. <https://doi.org/10.1126/science.aad2333>
- De Andrade Salgado, F., de Andrade Silva, F., (2022). Recycled aggregates from construction and demolition waste towards an application on structural concrete: A review. *Journal of Building Engineering* 52, 104452. <https://doi.org/10.1016/J.JOBE.2022.104452>
- Del Coz Díaz, J.J., García Nieto, P.J., Rodríguez, A.M., Martínez-Luengas, A.L., Biempica, C.B., (2006). Non-linear thermal analysis of light concrete hollow brick walls by the finite element method and experimental validation. *Appl Therm Eng* 26, 777–786. <https://doi.org/10.1016/J.APPLTHERMALENG.2005.10.012>
- Ding, T., Xiao, J., Zou, S., Wang, Y., (2020). Hardened properties of layered 3D printed concrete with recycled sand. *Cem Concr Compos* 113, 103724. <https://doi.org/10.1016/j.cemconcomp.2020.103724>
- Freitas, J. de S., Cronemberger, J., Soares, R.M., Amorim, C.N.D., (2020). Modeling and assessing BIPV envelopes using parametric Rhinoceros plugins Grasshopper and Ladybug. *Renew Energy* 160, 1468–1479. <https://doi.org/10.1016/j.renene.2020.05.137>
- Goode, A.H., Tyrrell, M.E., Feld, I.L., (1972). Glass wool from waste glass. US Department of Interior, Bureau of Mines.
- Gustafsson, S.E., (1991). Transient plane source techniques for thermal conductivity and thermal diffusivity measurements of solid materials. *Review of Scientific Instruments* 62, 797–804. <https://doi.org/10.1063/1.1142087>
- Han, Y., Yang, Z., Ding, T., Xiao, J., (2021). Environmental and economic assessment on 3D printed buildings with recycled concrete. *J Clean Prod* 278, 123884. <https://doi.org/10.1016/J.JCLEPRO.2020.123884>
- Han, Y., Yang, Z., Ding, T., Xiao, J., (2020). Environmental and Economic Assessment on 3D Printed Buildings with Recycled Concrete. *J Clean Prod* 278, 123884. <https://doi.org/10.1016/j.jclepro.2020.123884>
- Jeffrey, C., (2011). Construction and demolition waste recycling: A literature review. *Dalhousie University's Office of Sustainability* 35.

- Jianming, Y., Luming, W., Cheng, J., Dong, S., (2020). Effect of fly ash on the corrosion resistance of magnesium potassium phosphate cement paste in sulfate solution. *Constr Build Mater* 237, 117639. <https://doi.org/10.1016/j.conbuildmat.2019.117639>
- Le Duigou, A., Correa, D., Ueda, M., Matsuzaki, R., Castro, M., (2020). A review of 3D and 4D printing of natural fibre biocomposites. *Mater Des* 194, 108911. <https://doi.org/10.1016/J.MATDES.2020.108911>
- Liu, H., Liu, C., Wu, Y., Bai, G., He, C., Zhang, R., Wang, Y., (2022). Hardened properties of 3D printed concrete with recycled coarse aggregate. *Cem Concr Res* 159, 106868. <https://doi.org/10.1016/J.CEMCONRES.2022.106868>
- Liu, Z., Li, M., Weng, Y., Wong, T.N., Tan, M.J., (2019). Mixture Design Approach to optimize the rheological properties of the material used in 3D cementitious material printing. *Constr Build Mater* 198, 245–255. <https://doi.org/10.1016/J.CONBUILDMAT.2018.11.252>
- Lopez Hurtado, P., Rouilly, A., Vandenbossche, V., Raynaud, C., (2016). A review on the properties of cellulose fibre insulation. *Build Environ* 96, 170–177. <https://doi.org/10.1016/j.buildenv.2015.09.031>
- Majumder, A., Canale, L., Mastino, C.C., Pacitto, A., Frattolillo, A., Dell'Isola, M., (2021). Thermal Characterization of Recycled Materials for Building Insulation. *Energies (Basel)* 14. <https://doi.org/10.3390/en14123564>
- Medina, N.F., Medina, D.F., Hernández-Olivares, F., Navacerrada, M.A., (2017). Mechanical and thermal properties of concrete incorporating rubber and fibres from tyre recycling. *Constr Build Mater* 144, 563–573. <https://doi.org/10.1016/J.CONBUILDMAT.2017.03.196>
- Ministero dello Sviluppo Economico: Roma, (2015). Decreto Ministeriale 26 Giugno 2015. Applicazione Delle Metodologie di Calcolo Delle Prestazioni Energetiche e Definizione Delle Prescrizioni e dei Requisiti Minimi Degli Edifici, Governo Italiano. Italy.
- Muthukrishnan, S., Kua, H.W., Yu, L.N., Chung, J.K.H., (2020). Fresh Properties of Cementitious Materials Containing Rice Husk Ash for Construction 3D Printing. *Journal of Materials in Civil Engineering* 32. [https://doi.org/10.1061/\(ASCE\)MT.1943-5533.0003230](https://doi.org/10.1061/(ASCE)MT.1943-5533.0003230)
- Panda, B., Lim, J.H., Tan, M.J., (2019). Mechanical properties and deformation behaviour of early age concrete in the context of digital construction. *Compos B Eng* 165, 563–571. <https://doi.org/10.1016/J.COMPOSITESB.2019.02.040>
- Qian, H., Hua, S., Yue, H., Feng, G., Qian, L., Jiang, W., Zhang, L., (2022). Optimizing the Application of Recycled Dust Powder in 3d Concrete Printing Materials Through Particle Densely Packing Theory. *SSRN Electronic Journal*. <https://doi.org/10.2139/ssrn.4079313>
- Ricciardi, P., Belloni, E., Cotana, F., (2014). Innovative panels with recycled materials: Thermal and acoustic performance and Life Cycle Assessment. *Appl Energy* 134, 150–162. <https://doi.org/10.1016/J.APENERGY.2014.07.112>
- Roussel, N., (2018). Rheological requirements for printable concretes. *Cem Concr Res* 112, 76–85. <https://doi.org/10.1016/J.CEMCONRES.2018.04.005>
- Sangiorgio, V., Parisi, F., Fieni, F., Parisi, N., (2022). The New Boundaries of 3D-Printed Clay Bricks Design: Printability of Complex Internal Geometries. *Sustainability* 14, 598. <https://doi.org/10.3390/su14020598>
- Streimikiene, D., Skulskis, V., Balezentis, T., Agnusdei, G.P., (2020). Uncertain multi-criteria sustainability assessment of green building insulation materials. *Energy Build* 219, 110021. <https://doi.org/10.1016/J.ENBUILD.2020.110021>
- Sun, S., Liu, R., Zhao, X., Zhang, Y., Yang, Y., (2019). Investigation on the water resistance of the fly-ash modified magnesium phosphate cement. *IOP Conf Ser Mater Sci Eng* 587, 12007. <https://doi.org/10.1088/1757-899X/587/1/012007>
- Ting, G.H.A., Tay, Y.W.D., Tan, M.J., (2021). Experimental measurement on the effects of recycled glass cullets as aggregates for construction 3D printing. *J Clean Prod* 300, 126919. <https://doi.org/10.1016/J.JCLEPRO.2021.126919>
- Tinoco, M.P., de Mendonça, É.M., Fernandez, L.I.C., Caldas, L.R., Reales, O.A.M., Toledo Filho, R.D., (2022). Life cycle assessment (LCA) and environmental sustainability of cementitious materials for 3D concrete printing: A systematic literature review. *Journal of Building Engineering* 52, 104456. <https://doi.org/10.1016/J.JOBE.2022.104456>
- Volpe, S., Petrella, A., Sangiorgio, V., Notarnicola, M., Fiorito, F., (2021a). Preparation and characterization of novel environmentally sustainable mortars based on magnesium potassium phosphate cement for additive manufacturing. *AIMS Mater Sci* 8, 640–658. <https://doi.org/10.3934/matserci.2021039>

- Volpe, S., Sangiorgio, V., Fiorito, F., n.d. (2022). Design of an efficient 3D printed envelope supported by parametric modelling, in: Colloqui.AT.e .Memoria e Innovazione.
- Volpe, S., Sangiorgio, V., Petrella, A., Coppola, A., Notarnicola, M., Fiorito, F., (2021b). Building Envelope Prefabricated with 3D Printing Technology. Sustainability 13. <https://doi.org/10.3390/su13168923>
- Xu, X., Lin, X., Pan, X., Ji, T., Liang, Y., Zhang, H., (2020). Influence of silica fume on the setting time and mechanical properties of a new magnesium phosphate cement. Constr Build Mater 235, 117544. <https://doi.org/10.1016/j.conbuildmat.2019.117544>
- Zhang, H., Xiao, J., (2021). Plastic shrinkage and cracking of 3D printed mortar with recycled sand. Constr Build Mater 302, 124405. <https://doi.org/10.1016/J.CONBUILDMAT.2021.124405>